Science Signaling
AAAS

www.sciencesignaling.org/cgi/content/full/4/192/ra62/DC1

Supplementary Materials for

Akt Determines Cell Fate Through Inhibition of the PERK-eIF2α Phosphorylation Pathway

Zineb Mounir, Jothi Latha Krishnamoorthy, Shuo Wang, Barbara Papadopoulou, Shirley Campbell, William J. Muller, Maria Hatzoglou, Antonis E. Koromilas*

*To whom correspondence should be addressed. E-mail: antonis.koromilas@mcgill.ca

Published 27 September 2011, *Sci. Signal.* **4**, ra62 (2011)
DOI: 10.1126/scisignal.2001630

This PDF file includes:

Other Supplementary Material for this manuscript includes the following:
(available at www.sciencesignaling.org/cgi/content/full/4/192/ra62/DC1)

Table S1 (Microsoft Excel format). Results of statistical analysis.

Materials and Methods

Drosophila RNAi and analysis

Primers (which incorporate a T7 promoter at the 5' and 3' ends) for dAkt/dPKB, dS6K, dPERK, and dGCN2 dsRNA synthesis were as follows: dAkt/dPKB forward primer: 5'GAATTAATACGACTCACTATAGGGAGAGTCAATAAACACAACTTTCGACCT; dAkt/dPKB reverse primer: 5'GAATTAATACGACTCACTATAGGGAGAGAATATTTGAGTGAAATGAGGAAC; dS6K forward primer: 5'GAATTAATACGACTCACTATAGGGAGACATCTACACAAACTGGGCATCA; dS6K reverse primer: 5'GAATTAATACGACTCACTATAGGGAGAGCTTAGCGTCGTATCATCAGGT; dPERK forward primer: 5'GAATTAATACGACTCACTATAGGGAGACGTATTGAATGCATCGGAGTT; dPERK reverse primer: 5'GAATTAATACGACTCACTATAGGGAGACTGAAAGCGGGAAGTGTAATG; dGCN2 forward primer: 5'GAATTAATACGACTCACTATAGGGAGATGGAGCAGCGAGTCAAAGTG; dGCN2 reverse primer: 5'GAATTAATACGACTCACTATAGGGAGACGTAAAAGCGTAAGAATGGATG; TfR forward primer: 5'GAATTAATACGACTCACTATAGGGAGAAGCTGGGACGGTGGTGACTTTG; TfR reverse primer: 5'GAATTAATACGACTCACTATAGGGAGACGTTGAGGTTCCCGATGTGC. The underlined region indicates the T7 promoter sequence. dsRNA products were purified with the T7 MEGAscript RNAi kit (Ambion).

Side-directed mutagenesis

A plasmid containing the complementary DNA (cDNA) encoding wild-type Myc-PERK was subjected to mutagenesis resulting in a threonine (T) 799 to alanine (A) mutation with the QuikChange XL site-directed mutagenesis kit (Stratagene) and verified by sequencing. Primer sequences are as follows: T799A forward primer: 5'-GTCTAGGGAAGGAGCGTCCTCCTCCATAG-3'; T799A reverse primer: 5'CTATGGAGGAGGACGCTCCTTCCCTAGAC-3'. The mutation was confirmed by sequencing of the entire cDNA encoding PERK T799A.

Detection of XBP-1 mRNA splicing by RT-PCR

Total RNA was isolated from U87 glioblastoma cells that were untreated or were treated with LY294002 (20 μM) or thapsigargin (1 μM) with the TRIzol reagent (Invitrogen) as specified by the manufacturer. The splicing of hXBP-1 was detected by standard RT-PCR with the hXBP-1-specific primers hXBP1.3S (5′-AAACAGAGTAGCAGCTCAGACTGC-3′) and hXBP1.12AS (5′-TCCTTCTGGGTAGACCTCTGGGAG-3′). The RT step was performed as follows: 70°C for 10 min; 62°C for 2.5 min; 42°C for 1.5 hours, 95°C for 10 min, and then incubated 4°C. The PCR step was performed as follows: 94°C for 4 min followed by 35 cycles at 94°C for 10 s, 65°C for 30 s, and 72°C for 30 s, followed by a final step at 72°C for 10 min. DNA digestion was performed with Pst 1 for 1 hour at 37°C. Amplified

cDNAs were separated by electrophoresis on 2% agarose gels and visualized by ethidium bromide staining.

Purification of GST-fusion proteins

Seed cultures of BL-21 cells expressing GST-PERK K618A or GST-GSK3β K85R/K86R constructs were grown overnight at 37°C with shaking, and used to inoculate large cultures (1:100) the following day. Large cultures were induced with isopropyl-β-D-1-thiogalactopyranoside (IPTG, 0.1 mM) for 3 hours as soon as the OD_{600} of the cultures reached ~0.8. Bacterial cells were pelleted, washed, and sonicated, and proteins were solubilized with 1% (v/v) Triton X-100 at 4°C for 30 min. Lysates were centrifuged, and fusion proteins were purified by pulldown with glutathione (GSH) sepharose beads (Amersham) for 1 hour at 4°C.

Mass spectrometric analysis

Proteins were extracted from SDS-PAGE gels, placed in 96-well plates, and then washed with water. Tryptic digestion was performed on a MassPrep liquid handling robot (Waters) according to the manufacturer's specifications and to previously published protocols (*1*, *2*). Briefly, proteins were reduced with dithiothreitol (DTT, 10 mM) and alkylated with iodoacetamide (55 mM). Trypsin digestion was performed with modified porcine trypsin (Sequencing grade, 105 mM, Promega) at 58°C for 1 hour. Digestion products were extracted with 1% formic acid, 2% acetonitrile, followed by 1% formic acid, 50% acetonitrile. The recovered extracts were pooled, dried in a vacuum centrifuge, and then resuspended in 8 μl of 0.1% formic acid, of which 4 μl were analyzed by mass spectrometry (MS). Peptide samples were separated by online reversed-phase (RP) nanoscale capillary liquid chromatography (nanoLC) and analyzed by electrospray mass spectrometry (ES MS/MS). The experiments were performed with a Thermo Surveyor MS pump connected to a LTQ linear ion trap mass spectrometer (ThermoFisher) equipped with a nanoelectrospray ion source (ThermoFisher). Peptide separation was performed on a PicoFrit column BioBasic C18, 10-cm × 0.075-mm internal diameter, (New Objective) with a linear gradient from 2 to 50% solvent B (acetonitrile, 0.1% formic acid) in 30 min, at 200 nl/min (obtained by flow-splitting). Mass spectra were acquired with a data-dependent acquisition mode with Xcalibur software version 2.0. Each full scan mass spectrum (400 to 2000 m/z) was followed by collision-induced dissociation of the seven most intense ions. The dynamic exclusion (30 s exclusion duration) function was enabled, and the relative collisional fragmentation energy was set to 35%. All MS/MS samples were analyzed with Mascot (Matrix Science, version 2.2.0). Mascot was set up to search the uniref100_14_7_Homo_sapiens database (98,018 entries) in which we added the PERK sequence with the assumption of trypsin digestion. Mascot was searched with a fragment ion mass tolerance of 0.50 Daltons and a parent ion tolerance of 2.0 Daltons. Iodoacetamide derivative of cysteine was specified as a fixed modification, and oxidation of methionine was specified as a variable modification as well as phosphorylation of serine, threonine, and tyrosine. One missed cleavage was allowed. Scaffold (version Scaffold-2_02_03, Proteome Software Inc.) was used to validate MS/MS–based peptide and protein identifications. Peptide identifications were accepted if they could be established at greater than 90.0% probability as specified by the Peptide Prophet algorithm (*3*). Protein identifications were accepted if they could be

established at greater than 95.0% probability and contained at least 2 identified peptides. Protein probabilities were assigned by the Protein Prophet algorithm (*4*). Proteins that contained similar peptides and could not be differentiated based on MS/MS analysis alone were grouped to satisfy the principles of parsimony. The phosphopeptide spectra were manually validated. A pronounced neutral loss of phosphoric acid from the precursor ion, fragment ion, or both was required as well as an extensive coverage of b and y series.

Transgenic mice, tissue harvesting, and histology

Transgenic mice carrying an oncogenic version of *ErbB-2* (NDL 2-5) under the MMTV promoter (MMTV/NDL) were interbred with separate strains of mice expressing activated Akt1 from the same mammary targeted promoter (MMTV/Akt1-DD), as previously described (5). Mammary tumor tissues were flash-frozen in nitrogen and lysates were prepared as previously described (5). Tissues were fixed in 10% buffered formalin and blocked in paraffin. Embedded tissues were sectioned at 4 μm and were stained with hematoxylin and eosin (H&E) stain.

Immunohistochemistry

To detect pPERK T980, tissue samples were sectioned at 4 μm, placed on charged slides, air-dried, and loaded onto the Discovery XT Autostainer (Ventana Medical Systems). All solutions used for automated immunohistochemistry were from Ventana Medical System unless otherwise specified. Slides underwent de-paraffinization, heat-induced epitope retrieval (CC1 solution, mild protocol). Immunostaining for pPERK was performed online using a heat protocol. Briefly, rabbit monoclonal antibody against pPERK (Thr^{980}) (Cell Signaling Technology) diluted 1:50 in 5% normal goat serum (NGS) was manually applied for 32 min at 37°C, which was then followed by the appropriate detection kit (Omnimap anti-Rabbit HRP). A negative control was performed by the omission of the primary antibody. Slides were counterstained with hematoxylin for four minutes, incubated with Bluing Reagent for four minutes, removed from the autostainer, washed in warm soapy water, dehydrated through graded alcohols, cleared in xylene, and mounted with Permount. Immunoperoxidase staining for p-Akt S473 (Cell Signaling Technology) was performed by the avidin-biotin complex method (Vector Laboratories). Formalin-fixed paraffin embedded sections (4-μm) were cut, placed on SuperFrost/Plus slides (Fisher), and dried overnight at 37°C. Sections were deparaffinized in xylene and rehydrated through graded alcohols to water. Sections were immersed in 10 mM sodium citrate buffer (pH 6.0), and subjected to heat-induced antigen retrieval. Endogenous peroxidase activity was quenched by incubation in 3% hydrogen peroxide for 15 min. Endogenous biotin was blocked by incubation for 10 min with the Avidin/Biotin blocking kit (Zymed Laboratories Inc.). To block nonspecific protein binding, sections were then treated with 5% NGS in tris-buffered saline (TBS) containing Tween 0.1% (TBS-T) for 60 min at room temperature. Sections were incubated overnight at 4°C with primary antibodies at the appropriate dilutions in TBS-T with 5% NGS: rabbit monoclonal antibody against pAKT at a 1:35 dilution (Cell Signaling Technology, Inc.). After rinsing with TBS-T, sections were incubated with biotinylated antibody (goat antibody against rabbit Ig, Vector Laboratories) for 60 min at room temperature. The sections were then incubated for 30 min with avidin-biotin-horseradish peroxidase complex (Vector

Laboratories), followed by final color development with the peroxidase substrate kit DAB (Vector Laboratories) for 3 to 5 min. A negative control was performed by the omission of the primary antibody. Sections were then lightly counterstained with hematoxylin, dehydrated in graded alcohols, cleared in xylene, and prepared on cover-slips. Sections were analyzed by conventional light microscopy.

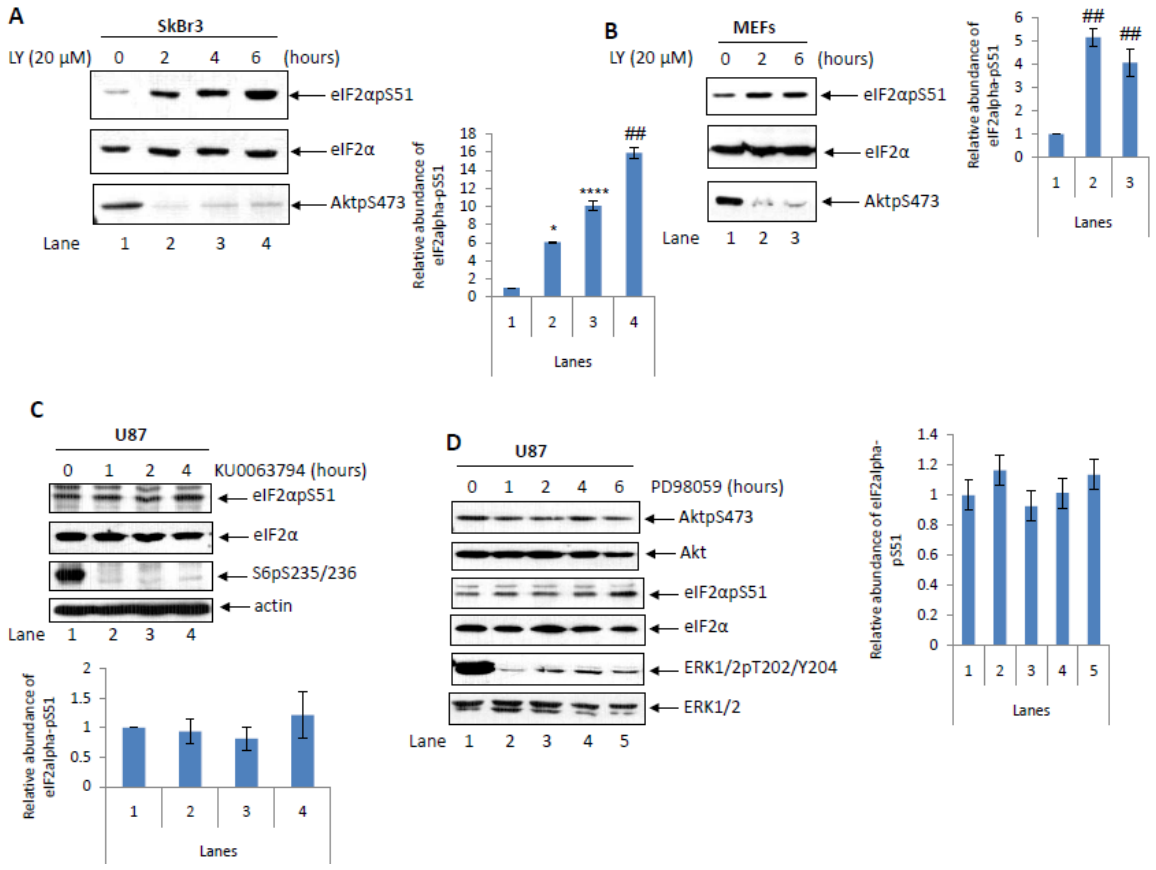

Fig. S1. Specificity of induction of eIF2αP by PI3K inhibitors. Human breast cancer SkBr3 cells (**A**) or immortalized mouse embryonic fibroblasts (MEFs) (**B**) were left untreated (A and B, lane 1) or treated with 20 μM LY294002 (A, lanes 2 to 4; B, lanes 2 to 3) for the indicated times. (**C**) Human glioblastoma U87 cells were left untreated (lane 1) or treated with 1 μM KU0063794 (lanes 2 to 4) for the indicated times. (**D**) U87 cells were left untreated (lane 1) or were treated with 50 nM PD98059 (lanes 2 to 5) for the indicated times. (A to D) Protein extracts (50 μg) were analyzed by Western blotting for the indicated proteins. The ratio of the abundance of eIF2αP to that of total eIF2α for each lane is indicated in the bar graphs that accompany each panel. Data are representative of three experiments. Error bars indicate the standard deviation (SD). In this and all other figures, symbols that define statistical significance are as follows: ####, $P < 0.05$; ###, $P < 0.01$; ##, $P < 0.005$; #, $P < 0.002$; ****, $P < 0.001$; ***, $P < 0.0005$; **, $P < 0.0002$; *, $P < 0.0001$. A list of the statistical comparisons in each figure can be found in table S1.

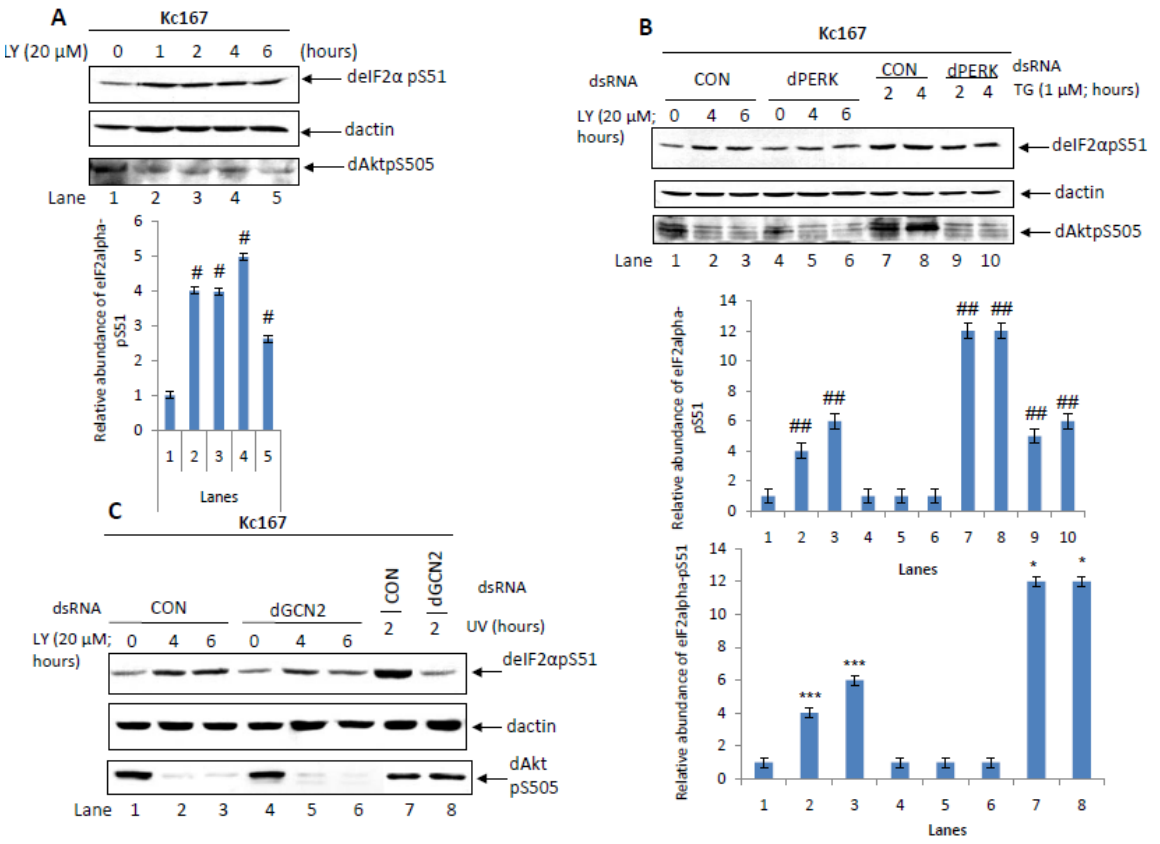

Fig. S2. Induction of eIF2α phosphorylation by PI3K inhibition in *Drosophila* cells. (**A**) *Drosophila* Kc167 embryonic cells were left untreated (lane 1) or wer treated with 20 μM LY294002 (lanes 2 to 5) for the indicated times. (**B** and **C**) Kc167 cells were treated with dsRNA against human transferrin receptor as negative control (B, lanes 1 to 3,7, and 8; C, lanes 1 to 3 and 7), dPERK (B, lanes 4 to 6, 9, and 10), or dGCN2 (C, lanes 4 to 6 and 8) in the absence (B and C, lanes 1 and 4) or presence of 20 μM LY294002 (B and C, lanes 2, 3, 5, and 6), 1 μM thapsigargin (TG) (B, lanes 7 to 10) or UV-C irradiation ($20J/m^2$) (C, lanes 7 and 8) for the indicated times. (A to C) Protein extracts (50 μg) were analyzed by Western blotting for the indicated proteins. The ratio of the abundance of deIF2αP to dactin for each lane is indicated in the bar graphs that accompany each panel. Data are representative of three experiments. Error bars indicate the SD.

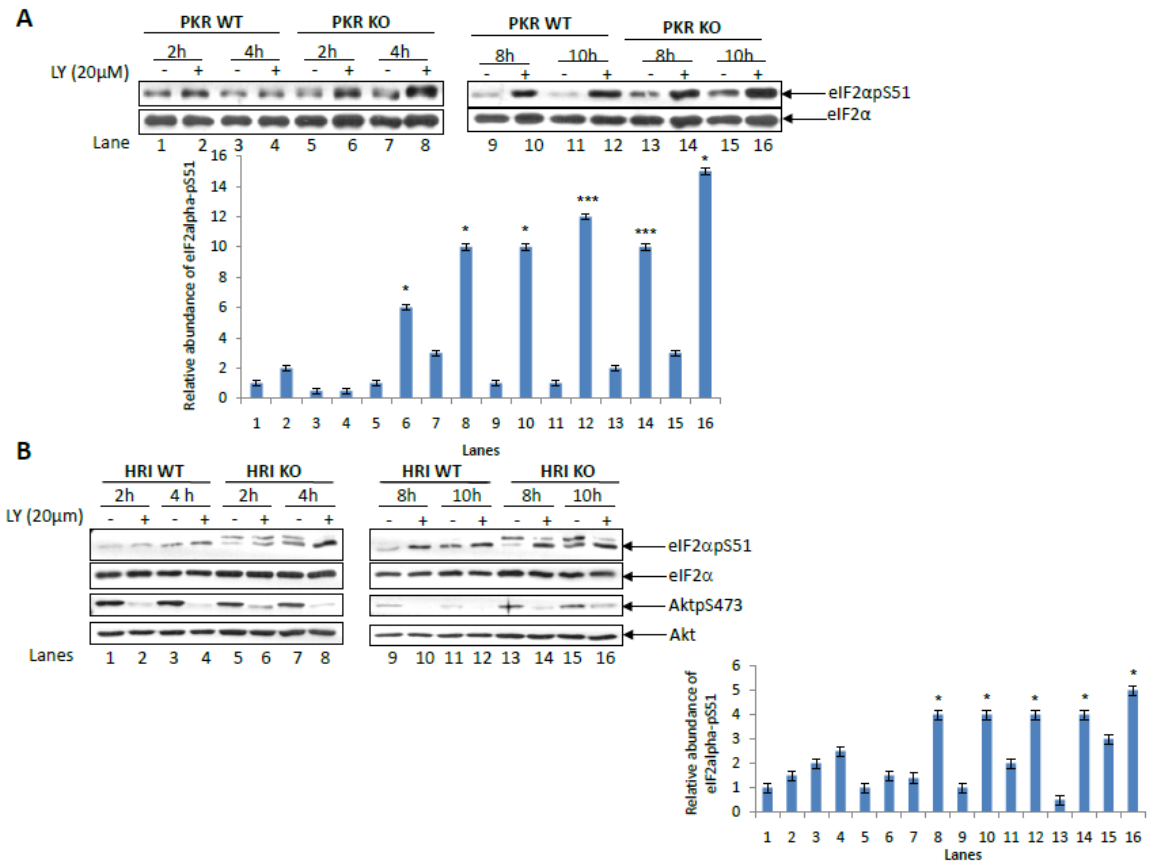

Fig. S3. PKR and HRI are not involved in the induction of eIF2α phosphorylation by PI3K inhibition. (**A**) Isogenic PKR wild-type (WT) and PKR KO MEFs and (**B**) HRI WTand HRI KO MEFs were left untreated (A and B, lanes 1, 3, 5, 7, 9, 11, 13, and 15) or were treated with 20 μM LY294002 (A and B, lanes 2, 4, 6, 8, 10, 12, 14, and 16) for the indicated times. (A and B) Protein extracts (50 μg) were analyzed by Western blotting for the indicated proteins. The ratio of the abundance of eIF2αP to that of total eIF2α as well as that of pAkt to total Akt for each lane is indicated in the bar graphs that accompany each panel. Data are representative of three experiments. Error bars indicate the SD.

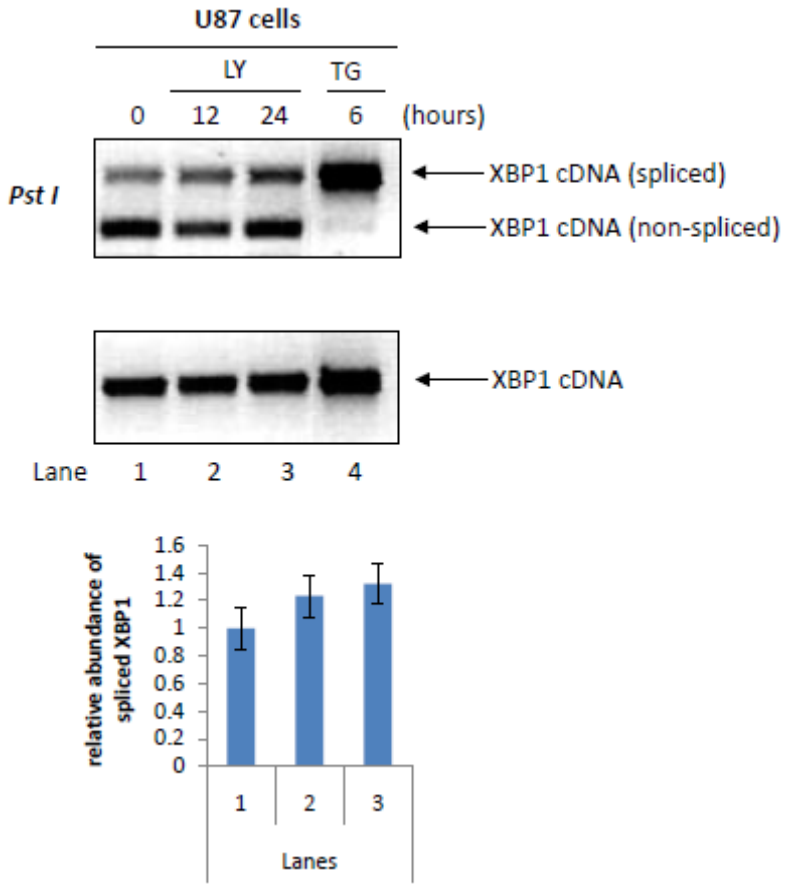

Fig. S4. PI3K inhibition does not result in induction of ER stress. Human glioblastoma U87 cells were left untreated (lane 1) or were treated with either 20 μM LY294002 (lanes 2,3) or 1 μM thapsigargin (TG) (lane 4) for the indicated times. Total RNA (1 μg) was subjected to RT-PCR analysis to detect XBP1 mRNA splicing, as described earlier. The amplified XBP-1 cDNA (bottom panel) was subjected to digestion with Pst I to distinguish between cDNAs that arose from spliced and unspliced XBP-1 mRNA (top panel). The ratio between the spliced and un-spliced form of XBP-1 mRNA for each lane is indicated in the bar graph. Data are representative of three experiments. Error bars indicate the SD.

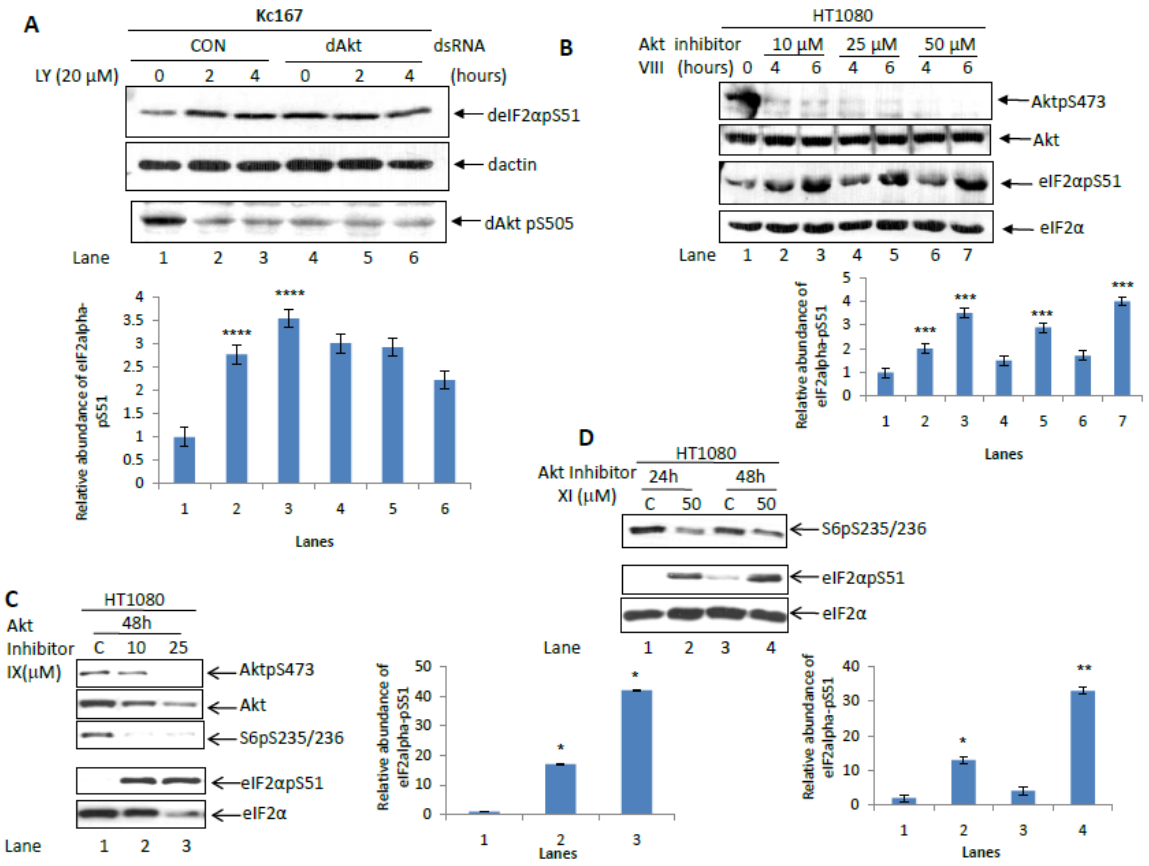

Fig. S5. Akt inactivation results in the induction of eIF2α phosphorylation. (**A**) *Drosophila* Kc167 cells were treated with control dsRNA against human transferrin receptor as negative control (lanes 1 to 3) or dAkt (lanes 4 to 6) in the absence (lanes 1 and 4) or presence of 20 μM LY294002 (lanes 2, 3, 5, and 6) for the indicated times. (**B** to **D**) Human fibrosarcoma HT1080 cells were treated with increasing concentrations of (B) Akt inhibitor VIII or (C) Akt inhibitor IX or with (D) 50 μM Akt inhibitor XI for the indicated times. (A to D) Protein extracts (50 μg) were analyzed by Western blotting for the indicated proteins. The ratio of the abundance of (d)eIF2αP to that of total eIF2α or dactin for each lane is indicated in the bar graphs that accompany each panel. Data are representative of three experiments. Error bars indicate the SD.

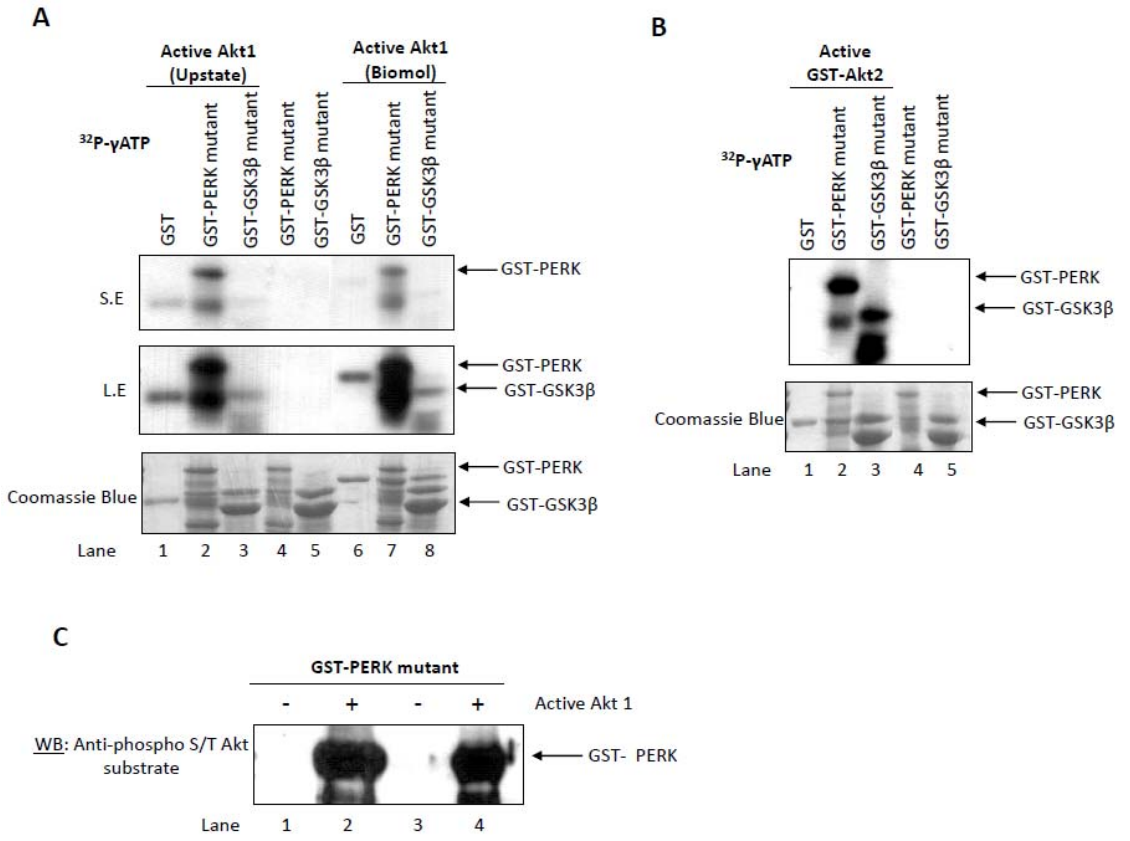

Fig. S6. PERK is phosphorylated by Akt in vitro. (**A**) GST-fusion proteins (~500 ng) encompassing either the cytoplasmic domain of the catalytically inactive (K618A) mutant of mouse PERK (lanes 2 and 7) or full-length catalytically inactive GSK-3β bearing the K85R/K86R mutations (lanes 3 and 8) were subjected to in vitro phosphorylation by active Akt1 (1 μg) obtained from two different commercial sources (Upstate, lanes 1 to 3; Biomol, lanes 6 to 8). As a control, an equivalent amount of GST alone was incubated with active Akt1 (lanes 1 and 6) or equivalent amounts of catalytically inactive mutants of GST-PERK and GST-GSK-3β were subjected to in vitro phosphorylation in the absence of active Akt1 (lanes 4 and 5). Protein phosphorylation assays were performed as described earlier. Phosphorylated proteins were subjected to SDS-PAGE and autoradiography (S.E., short exposure; L.E. long exposure). The GST-fusion proteins were visualized by Coomassie blue staining of the SDS-PAGE gel. The positions of the phosphorylated proteins are indicated with arrows. (**B**) Purified GST-fusion proteins as described in (A) were subjected to in vitro kinase assay with 1 μg of active GST-Akt2 (Biomol). Protein phosphorylation was detected by autoradiography (top panel), whereas the amounts of GST-fusion proteins were detected by Coomassie blue staining (bottom panel). (**C**) GST-PERK K618A was subjected to an in vitro kinase assay with active Akt1 from two different sources in the presence of non-radioactive ATP as described in the Materials and Methods. Phosphorylation of GST-PERK was detected by Western blotting analysis with antibody against Akt substrates with pSer and pThr residues.

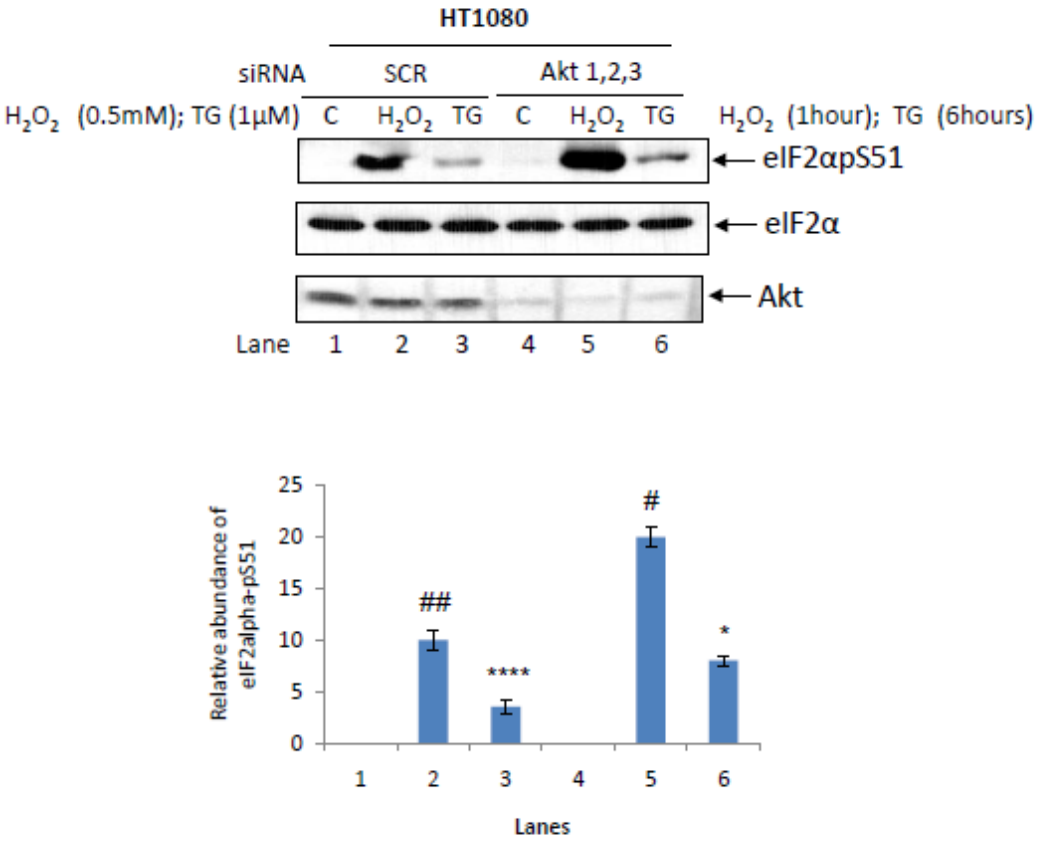

Fig. S7. Akt diminishes the induction of eIF2α phosphorylation in response to oxidative or ER stress in human cells. Human fibrosarcoma HT1080 cells were treated with either scrambled control siRNA (lanes 1 to 3) or siRNA against Akt1, 2, and 3 (lanes 4 to 6). Cells were then treated with either 0.5 mM H_2O_2 for 1 hour (lanes 2 and 5) or 1 μM thapsigargin (TG) for 6 hours (lanes 3 and 6). Protein extracts (50 μg) were analyzed by Western blotting for the indicated proteins. The ratio of the abundance of eIF2αP to that of total eIF2α is indicated for each lane in the bar graph. Data are representative of three experiments. Error bars indicate the SD.

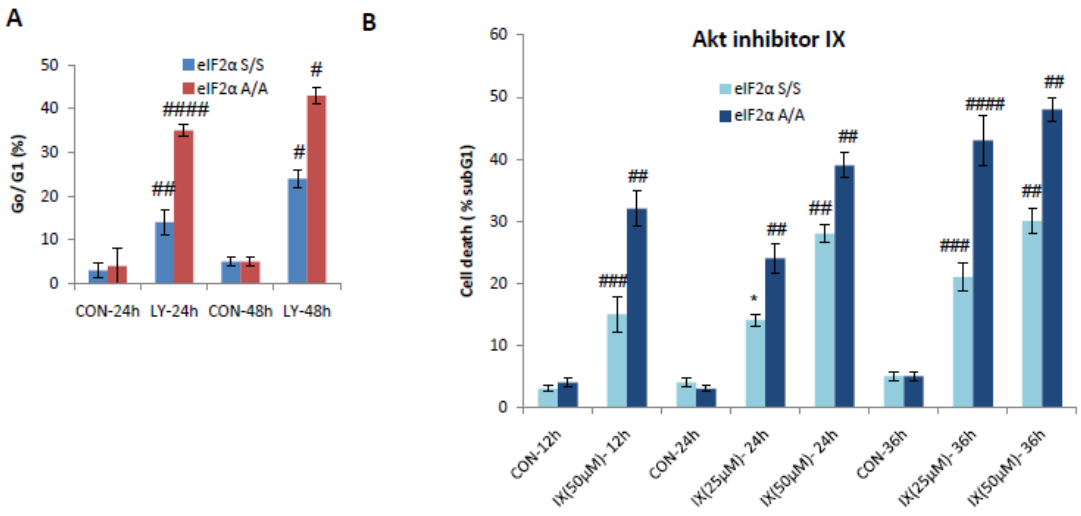

Fig. S8. Induction of PERK activation and eIF2α phosphorylation by PI3K or Akt inactivation promotes cell survival. Isogenic eIF2α S/S and eIF2α A/A MEFs were treated with (**A**) 20 μM LY294002 for 24 or 48 hours or (**B**) 50 μM Akt inhibitor IX for 12, 24, or 36 hours. Cell cycle arrest (% of cells in G_0/G_1) levels compared to untreated cells plated the previous day (**A**) or cell death (% of cells $subG_1$) (**B**) was assessed by propidium iodide staining and flow cytometric analysis. Data are representative of three experiments. Error bars indicate the SD.

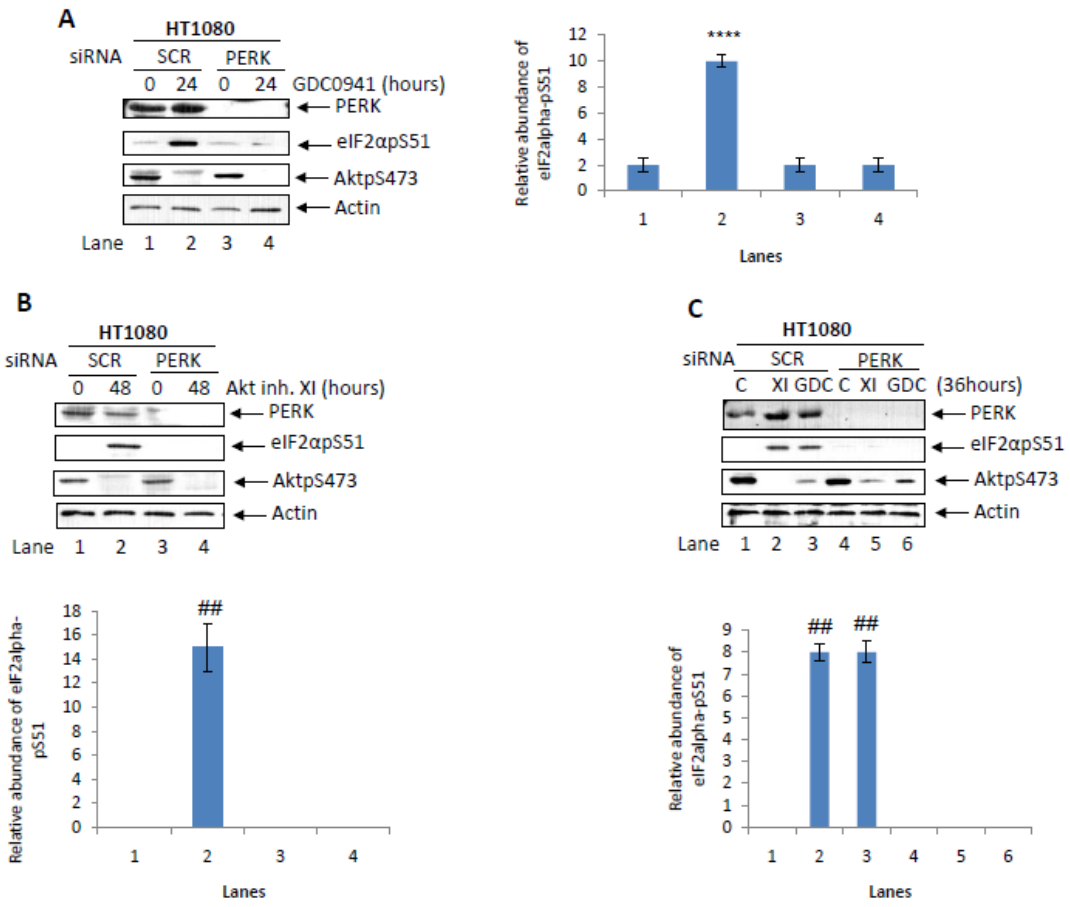

Fig. S9. Inactivation of PERK increases the efficacy of tumor treatment with PI3K and Akt inhibitors. (**A** to **C**) HT1080 cells were treated with scrambled control siRNA or siRNA against PERK in the absence or presence of (A and C) 10 μM GDC-0941 or (B and C) 50 μM Akt inhibitor XI for the indicated times. Protein extracts (50 μg) were analyzed by Western blotting for the indicated proteins. Data are representative of two experiments. Error bars indicate the SD.

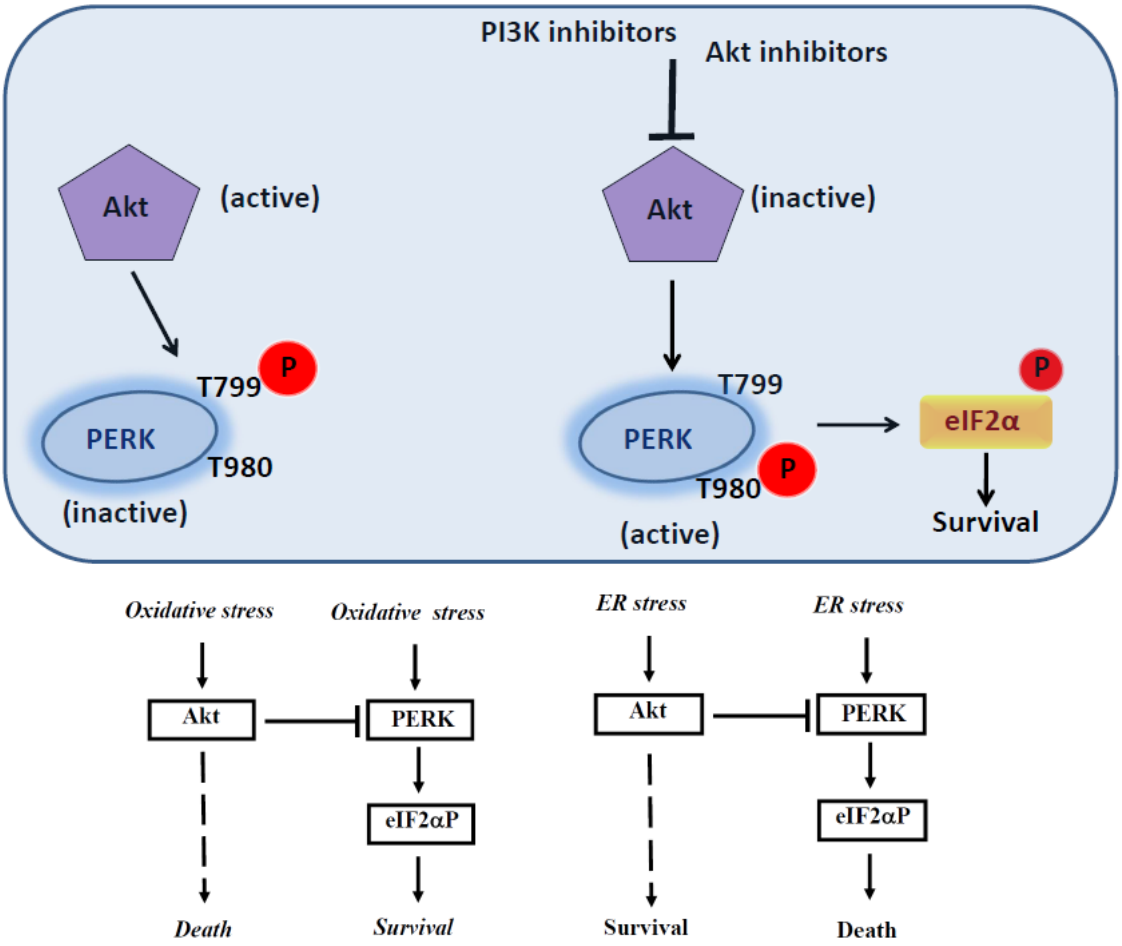

Fig. S10. Model of the inhibition of the PERK-eIF2αP arm by Akt. *Top panel* In unstressed and proliferating cells, Akt maintains PERK activity and eIF2α phosphorylation to a low extent through phosphorylation of PERK at Thr^{799} (T799, left arm). Treatment of cells with pharmacological inhibitors of the PI3K-Akt pathway, as well as genetic ablation of Akt, results in decreased PERK phosphorylation at Thr^{799}, which in turn activates PERK by autophosphorylation at Thr^{980} resulting in the induction of eIF2α phosphorylation (right arm). Under conditions of disruption of the PI3K-Akt pathway, the induction of eIF2α pathway promotes cell survival and represents a "back up" mechanism used by cells to adapt to disruption of the PI3K-Akt pathway (right arm). *Bottom panel* Under stress, PERK and eIF2αP act as antagonists of Akt function, that is, the PERK-eIF2αP arm impedes both the pro-apoptotic effects of Akt in response to oxidative stress and the pro-survival effects of Akt in cells in response to prolonged ER stress. Under these conditions, PERK phosphorylation at Thr^{799} is a feedback mechanism used by Akt to promote its function by neutralizing PERK activity and eIF2α phosphorylation.

References

1. A. Shevchenko, M. Wilm, O. Vorm, M. Mann, Mass spectrometric sequencing of proteins silver-stained polyacrylamide gels. *Anal. Chem.* **68**, 850–858 (1996).
2. J. Havlis, H. Thomas, M. Sebela, A. Shevchenko, Fast-response proteomics by accelerated in-gel digestion of proteins. *Anal. Chem.* **75**, 1300–1306 (2003).
3. A. Keller, A. I. Nesvizhskii, E. Kolker, R. Aebersold, Empirical statistical model to estimate the accuracy of peptide identifications made by MS/MS and database search. *Anal. Chem.* **74**, 5383–5392 (2002).
4. A. I. Nesvizhskii, A. Keller, E. Kolker, R. Aebersold, A statistical model for identifying proteins by tandem mass spectrometry. *Anal. Chem.* **75**, 4646–4658 (2003).
5. J. N. Hutchinson, J. Jin, R. D. Cardiff, J. R. Woodgett, W. J. Muller, Activation of Akt-1 (PKB-alpha) can accelerate ErbB-2-mediated mammary tumorigenesis but suppresses tumor invasion. *Cancer Res.* **64**, 3171–3178 (2004).